AO Performance model and error budget for GIRMOS

K Jackson[a], S Chapman[a,b,c], U Conod[a,b], C Correia[d,e], and G Sivo[f]

[a]NRC - Herzberg Astronomy and Astrophysics, 5711 West Saanich Rd, Victoria, BC, Canada
[b]Department of Physics and Astronomy, University of British Columbia, 6224 Agricultural Rd., Vancouver, BC, Canada
[c]Department of Physics and Atmospheric Science, Dalhousie University, Halifax, NS, B3H 4R2, Canada
[d]WM Keck Observatory
[e]Laboratoire d'Astrophysique de Marseille, 38 Rue Frédéric Joliot Curie, 13013 Marseille, France
[f]Gemini Observatory

ABSTRACT

The Gemini Infrared Multi-Object Spectrograph (GIRMOS) instrument proposes to carry out Multi-Object Adaptive Optics (MOAO) correction on the residual of the Gemini Mutlti-Conjugate AO System (GeMS)-corrected wavefronts in either Ground Layer (GLAO) or Multi-Conjugate (MCAO) mode. This work has been undertaken to determine the extent to which the ensquared energy delivered to a GIRMOS IFU can be improved over typical GeMS operation by adding MOAO correction. One of the key advantages of using the MOAO-fed IFUs is the improvement in performance toward the edge of the field, making the full 2' field of GeMS more available for simultaneous observing. Using the Object Oriented Matlab Adaptive Optics (OOMAO) library[1] to simulate the full system under a wide range of configurations and error conditions, we have established the baseline error budget and used the simulation to enable ongoing investigation into the particular control schemes and system errors that arise from using GeMS LGS and NGS WFSs to divide atmospheric correction between up to 3 DMs at different altitude conjugations and optimization directions.

1. INTRODUCTION

GIRMOS is an AO-fed multi-object spectrograph which has recently passed its conceptual design review.[2] This paper describes the open loop AO error budget and performance estimates at the IFU focal plane. This paper is divided into 4 sections. Section 2 is a complete description of the baseline end-to-end simulation and a series of results showing the idealized GIRMOS performance in contrast to GeMS in both GLAO and MCAO mode. Section 3 gives the methodology and results of the analytic high order (Tip/Tilt removed) error budget development. Section 4 describes the Tip/Tilt control strategy for GIRMOS, as well as some sample simulation cases to demonstrate proper agreement. Section 5 outlines the results of some detailed investigations into the impact of known issues with the GeMS LGS WFS measurement data on the MOAO performance.

2. BASELINE SIMULATION

The simulation effort has been focused on two primary objectives: Showing that improvement can be made in ensquared energy (EE) by adding MOAO correction to the residual wavefronts provided by a wide field AO system operating in GLAO or MCAO mode, and injecting the realistic aspects of the particular performance delivered by the GeMS LGS WFSs. In the first objective, a systematic analytical approach to identifying and quantifying the major error terms has been combined with an end-to-end simulation of GeMS+GIRMOS. In the second objective, the end-to-end simulation has been used to study the impacts of LGS WFS error sources on both GeMS and GIRMOS performance. The baseline simulation parameters are given in Table 1, and the arrangement of the LGS, NGS and science objects are shown in Fig. 1.

Further author information: (Send correspondence to K Jackson)
K Jackson: E-mail: kathryn.jackson@nrc-cnrc.gc.ca

Table 1. Baseline simulation parameters.

Telescope	
Diameter	8 m
Obstruction ratio	0.14
Atmosphere	
r_0 (500nm)	15.5 cm
L_0	40 m
Layer altitudes	0, 5.5, 11.5 km
Fractional r_0	0.6, 0.22, 0.18
Wind speeds	5.7, 6, 17 m/s
Open Loop DM	
Order	17x17
Coupling	0.4
Pitch	0.5m
Wavefront Sensors	
Order	16x16
N LGS	5
LGS asterism	(0,0) + 1' square
Npix/lenslet	12
θ_{pix}	0.17" (FoV = GeMS quadcell)
framerate	500 Hz
λ	589 nm
LGS mag	12
N Tip/Tilt stars	1 or 3
Closed Loop DM	
Order	17x17
Coupling	0.33
Pitch	0.5m
Conjugation altitude	0 km
GeMS observing mode	GLAO or MCAO
Figure of Merrit	
Ensquared Energy	50%
Spaxel size	100 mas
λ	H-band ($1.65\mu m$)

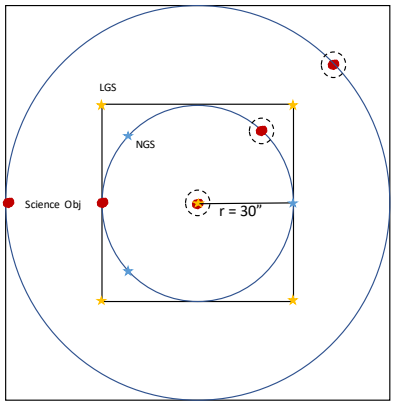

Figure 1. The baseline arrangement of the laser and natural guide stars, and some sampled science locations within the GeMS 2' FoV.

The ensquared energy has been computed in the idealized (noise-free) case for the three science directions indicated by dashed circles in Fig. 1, for three AO cases: GeMS in GLAO mode, GeMS in MCAO mode optimized over the whole 2' FoR, and GeMS in GLAO+GIRMOS MOAO. The EE as a function of spaxel size for each science location and AO mode are plotted in Fig. 2. This shows that GLAO+GIRMOS MOAO is improving over GeMS alone; it also shows that when MCAO is optimized over the full 2' FoR, it is not significantly different from GLAO on axis. Although MCAO is more uniform across the FoR by design, there is still significant improvement in EE when the MOAO step is added.

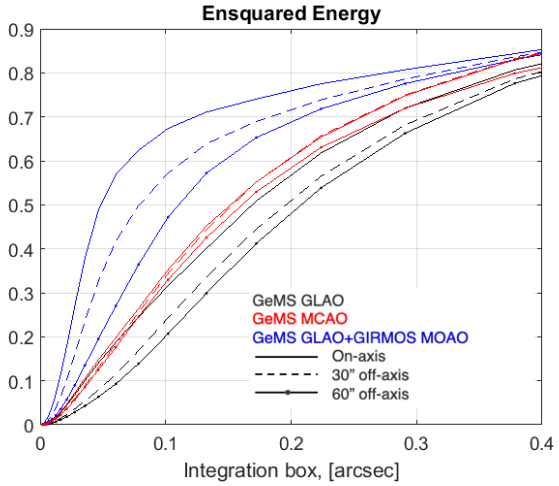

Figure 2. Idealized simulation of GeMS+GIRMOS compared to GeMS alone in GLAO and MCAO.

3. HIGH ORDER ERROR BUDGET

The analytic approach to creating the error breakdown in LGS MOAO described in[3] is combined with the OOMAO simulation to produce GIRMOS high order and Tip/Tilt WFE budget estimates.Tip/tilt removed tomographic error is computed using Eq. 3 with the GeMS asterism locations, α, over a series of field points, β, which represent 1/8th of the FoR. This is sufficient to represent the entire FoR due to symmetry. The GIRMOS MOAO baseline reconstructor is the zonal spatio-angular minimum-mean-square error solution which minimizes Eq. 1,

$$R_i = \arg\min_{R_i} \langle \| \overrightarrow{s_{\beta_i}} - R_i \widehat{s_{\beta_i}} \|^2 \rangle, \tag{1}$$

where $\overrightarrow{s_{\beta_i}}$ is the vector of slopes in β_i, the i^{th} science direction; R_i is the reconstructor to be solved for, and $\widehat{s_{\beta_i}}$ is the estimated slopes in the science direction. This matrix R_i is computed as in Eq. 2,

$$R_i = \Sigma_{\beta_i \overrightarrow{\alpha}} (\Sigma_{\overrightarrow{\alpha}\overrightarrow{\alpha}} + \Sigma_\eta)^{-1}, \tag{2}$$

where $\overrightarrow{\alpha}$ is the vector of LGS directions, and Σ_η is the noise covariance matrix. The cross and auto-correlation between all of these locations at each altitude, Σ, and the reconstructor, R, computed for each field point, are used to compute the tomographic error variance,

$$\sigma^2_{Tomo} = tr\{\Sigma_{\beta\beta} - \Sigma_{\beta\alpha} R^T - R\Sigma^T_{\beta\alpha} + R\Sigma_{\alpha\alpha} R^T\}. \tag{3}$$

The resulting tomographic error map is shown in Figure 3.

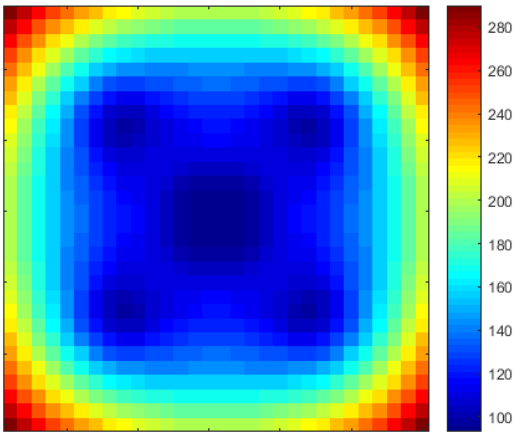

Figure 3. Tip/Tilt removed tomographic error computed using Eq. 2. The map covers the full 2' FoR, with the LGSs placed as shown in Fig. 1; the colour scale is nm RMS of wavefront error.

The DM fitting error is approximated from

$$\sigma^2_{fit} \approx 0.23 \left(\frac{d_{act}}{r_0}\right)^{5/3}, \tag{4}$$

were d_{act} is the actuator pitch on sky (0.5m), and 0.23 is a factor derived from the actuator coupling.

Aliasing error is the amount of unmeasurable and uncorrectable high spatial frequencies incorrectly mapped onto lower frequencies,

$$\sigma^2_{Alias} = tr\{R\Sigma^{Alias}_{\alpha\alpha} R^T\}, \tag{5}$$

were the aliasing covariance matrix is the covariance of the atmospheric spatial frequencies above the cut-off frequency of the DM.

Noise error is computed from a simulated noise covariance matrix, $\Sigma^{noise}_{\alpha\alpha}$. This term includes photon noise, assuming an LGS return of $1.6x10^4 \gamma/m^2/s$ at 500Hz, and camera readout noise of $3e^-$,

$$\sigma^2_{noise} = \eta tr\{R\Sigma^{noise}_{\alpha\alpha} R^T\}, \qquad \eta = \frac{g_{OL}}{2 - g_{OL}}, \tag{6}$$

where g_{OL} is the open loop gain on the MOAO correction loop.

A pessimistic estimate of $\epsilon = 0.05$ (5%) is used for the amount of stroke taken up by go-to errors in the OL-DM; these can include effects such as hysteresis, non-linearity and creep. The variance is computed using Eq. 7, and is independent of science direction.

$$\sigma^2_{goto} = (\epsilon/2)^2 tr\{R\Sigma_{\alpha\alpha} R^T\} \tag{7}$$

The results of these computations are shown in Tab. 2; in the case of direction-dependant errors, the average over the 2' diameter circular FoV is given.

Table 2. High order error budget breakdown.

Error Term	WFE [nm RMS]
Tomographic (T/T Rem)	157
WFS Noise (LGS mag = 12, RON = 3e-)	44
Aliasing	67
OL DM Fitting	129
OL DM go-to	10
Total	208

4. TIP/TILT ERROR

GeMS MCAO operates with 3 T/T sensing 2x2 NGS SHWFSs. In the case of GIRMOS, and with the impending upgrade of the GeMS NGS WFSs to higher order SHWFSs, the sky coverage required by the majority of the science cases of interest would be greatly increased by the use of 2 or 1 NGS instead. An analytical estimate of the error due to T/T anisoplanatism in the case of a single NGS is computed using Eq. 8,

$$\sigma^2_{TA} = tr\{\Sigma_{\beta\beta} + \Sigma_{\alpha\alpha} - 2\Sigma_{\beta\alpha}\}. \tag{8}$$

To understand the impact of a T/T star's field location on wavefront error across the whole FoR, the T/T error variance was computed for a sample of science locations for a fixed NGS star located on axis, and in the case of a fixed NGS star at the corner of the FoR. The resulting RMS wavefront error for both cases is mapped in Fig. 4.

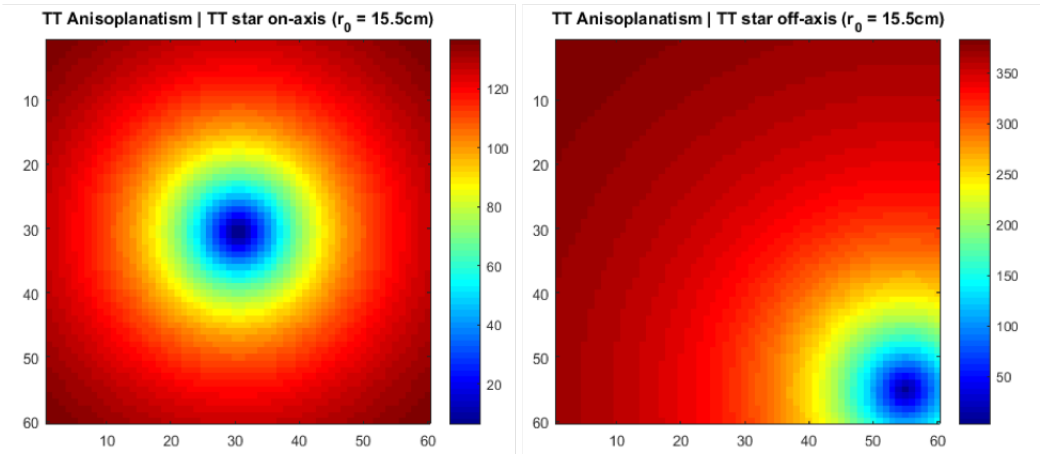

Figure 4. WFE due to T/T anisoplanatism for a single NGS on axis (left) and off axis (right). The maps cover the full 2' FoR, and the colour scale is nm RMS of wavefront error.

To assess the impact on ensquared energy, the error variance was used to determine the width of a 2-D gaussian distribution which was convolved with the ideal (T/T error-free) PSF at that location. The results show the EE as a function of NGS location for a fixed science object (Fig. 5).

5. GEMS LGS WFS STUDIES

Three particular sources of error in the GeMS LGS WFSs have been identified as potentially detrimental to the performance of open loop AO. These are optical gain error, lenslet saturation (WFS linearity), and fratricide. Optical gain errors are caused by changing spot size due to the evolution of r_0 and of the mean altitude of the sodium layer. In an MCAO system the primary impact is on bandwidth and NCPA leakage. To mitigate NCPA error, it is proposed to use at least one of the figure WFSs in GIRMOS as an on-sky truth sensor whenever possible. It is proposed that this may be sufficient to gauge the NCPA leakage due to gain estimation errors for all 4 arms, possibly combined with a calibrated field dependent NCPA look-up table. This proposal has not yet

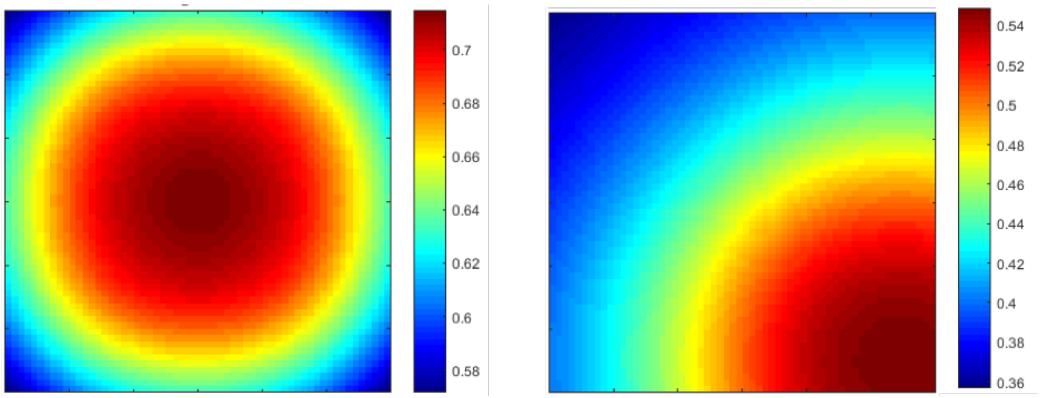

Figure 5. EE for a fixed science object location as a function of T/T star location in FoR. Science object on axis (left) and off axis (right). The maps cover the full 2' FoR, and the colour scale is EE in a 100mas spaxel, where a value of 1 is 100%.

Table 3. Performance summary with known GeMS LGS WFS errors present in various combinations.

AO Mode	Gain Error	Radial increase in gain error	Fratricide Mask	Slope Saturation	EE at 100mas
MCAO	±20%	20%	Yes	±0.5"	30.4%
GLAO+MOAO	-	-	No	-	62.0%
GLAO+MOAO	-	-	Yes	-	58.8%
GLAO+MOAO	-	-	No	±0.5"	55.7%
GLAO+MOAO	±20%	10%	No	-	51.2%
GLAO+MOAO	±20%	20%	No	-	45.3%
GLAO+MOAO	±20%	20%	Yes	-	43.1%
GLAO+MOAO	±20%	20%	Yes	±0.5"	41.3%

been simulated. The other major concern for OL AO using slopes with inaccurate gain estimates is the overall reduction in performance due to over and under-estimation of slope values with no optical feedback. A discrete-time varying gain error, $(g(t_i)_x, g(t_i)_y)$ has been incorporated into the simulation; due to spot elongation, the gain error induced by these changes varies with the radial and azimuthal position of each lenslet,

$$g_X = g(t_i)_x r_{LL} \cos\theta \tag{9}$$

$$g_Y = g(t_i)_y r_{LL} \sin\theta \tag{10}$$

If the latest gain estimate made by the GeMS controller is taken as truth, the question is how much error can be tolerated before the MOAO performance is too degraded. Taking the mean sodium layer thickness to be 10km, a 20% error corresponds to a delta of 2km.

To simulate lenslet saturation in the GeMS quadcells, the slopes are truncated at the end of the linear range. For a 1" spot size, saturation starts at slopes greater than ±0.5". Finally, the lenslets lost due to fratricide contamination are masked out in simulation as they would be in the GeMS system. The total number of masked lenslets is approximately 20%.

Taking all of these effects into account, a case study was made using a GSAOI image. A PSF was selected from the image, shown in Fig. 6, its location in the FoR was determined, and the EE in 100mas computed to be 26%. A simulation with a science object matching that location as well as the atmospheric conditions at the time of measurement was run with the WFS errors described above. The results are summarized in Tab. 3; it shows that the simulation of GeMS MCAO is over-performing by a small amount compared to the real image, and that the GLAO+MOAO mode of GIRMOS can still out-perform GeMS in MCAO despite the errors present.

Experience with GeMS observations has shown that often one WFS is saturated in T/T. In this case, it may be beneficial to discard the saturated WFS. The tomographic error map shown in Fig. 3 has been recomputed

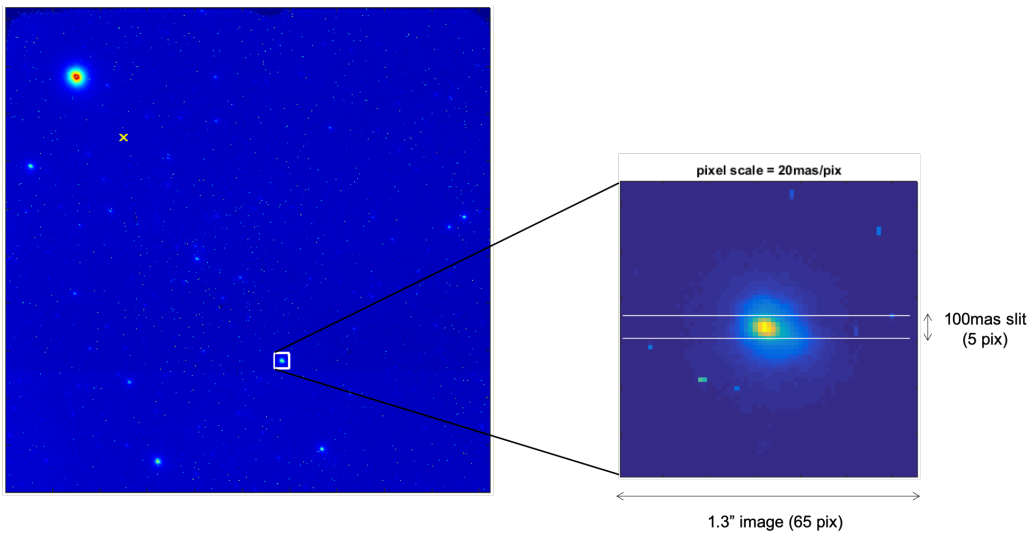

Figure 6. Engineering image taken with GSAOI and a particular PSF used for comparison with simulation results.

for the case where 4 LGSs are used instead of 5; one of the corner LGS WFSs has been discarded, as these are more likely to be saturated than the central WFS. The result of this computation is shown in Fig. 7, and the contours delimit the area of the FoR in which the performance is not worse than the 5 LGS case. The overall result is an area equal to approximately 12.5% of the total FoR sees worse performance.

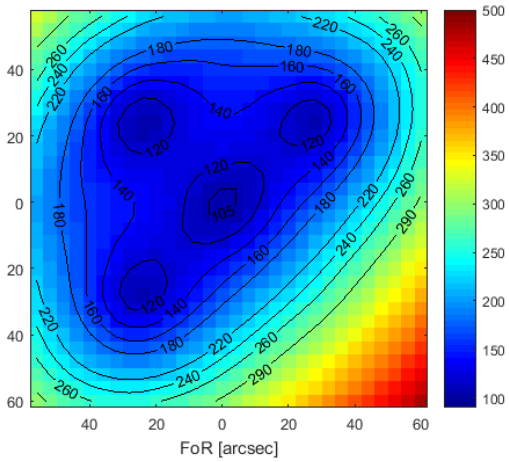

Figure 7. Tomographic error map with one LGS WFS dicarded due to T/T saturation. Contours show area of performance not worse than the 5 LGS case.The map covers the full 2' FoR, with the LGSs placed as shown in Fig. 1; the colour scale is nm RMS of wavefront error.

6. CONCLUSIONS

As we continue to identify and incorporate error sources particular to the GeMS/Gemini South system, the error budget will evolve. As it stands, the simulated MCAO performance is approaching the observed performance in EE. The estimated performance of GIRMOS in MOAO following GeMS in GLAO does not meet the figure of merit listed in Tab. 1 (50% EE in 100mas spaxel) under all conditions, but it is still predicting significant improvement, on the order of 15% in EE, over the existing system. The next step will be a focus on algorithms; the performance will be characterized using predictive reconstruction, including vibration suppression. Alternative WF reconstruction using residual slopes as opposed to POL slopes will also be considered.

7. ACKNOWLEDGEMENTS

The GIRMOS project gratefully acknowledges its financial support from the Canada Foundation for Innovation (CFI), Ontario Research Fund (ORF), British Columbia Knowledge Development Fund (BCKDF), Fonds de Recherche du Quebec (FRQ), Nova Scotia Research and Innovation Trust (NSRIT), University of Toronto and in-kind contributions from the National Research Council Canada (NRC) and the Association of Universities for Research in Astronomy (AURA) through its Gemini Observatory.

REFERENCES

[1] Conan, R. and Correia, C., "Object-oriented matlab adaptive optics toolbox," in [*Astronomical Telescopes + Instrumentation: Adaptive Optics Systems IV*], *Proc. SPIE* **9148**, 6C (2014).

[2] Sivanandam, S., Chapman, S., Simard, L., and et al, "Gemini infrared multi-object spectrograph: instrument overview," in [*Ground-based and Airborne Instrumentation for Astronomy VII*], *Proc. SPIE 10702* **10702**, 1J (2018).

[3] Martin, O., Gendron, E., Rousset, G., and et al, "Wavefront error breakdown in laser guide star multi-object adaptive optics validated on-sky by canary," *A&A* **A37**, 598 (2017).